

# Quantum back-action in measurements of zero-point mechanical oscillations

Farid Ya. Khalili,<sup>1</sup> Haixing Miao,<sup>2</sup> Huan Yang,<sup>2</sup> Amir H. Safavi-Naeini,<sup>3</sup> Oskar Painter,<sup>3</sup> and Yanbei Chen<sup>2</sup>

<sup>1</sup>*Physics Faculty, Moscow State University, Moscow 119991, Russia*

<sup>2</sup>*Theoretical Astrophysics 350-17, California Institute of Technology, Pasadena, California 91125, USA*

<sup>3</sup>*Thomas J. Watson, Sr. Laboratory of Applied Physics, California Institute of Technology, Pasadena, California 91125, USA*

(Received 8 June 2012; published 25 September 2012)

Measurement-induced back-action, a direct consequence of the Heisenberg uncertainty principle, is the defining feature of quantum measurements. We use quantum measurement theory to analyze the recent experiment of Safavi-Naeini *et al.* [*Phys. Rev. Lett.* **108**, 033602 (2012)], and show that the results of this experiment not only characterize the zero-point fluctuation of a near-ground-state nanomechanical oscillator, but also demonstrate the existence of quantum back-action noise—through correlations that exist between sensing noise and back-action noise. These correlations arise from the quantum coherence between the mechanical oscillator and the measuring device, which build up during the measurement process, and are key to improving sensitivities beyond the standard quantum limit.

DOI: 10.1103/PhysRevA.86.033840

PACS number(s): 42.50.Lc, 03.65.Ta, 42.50.Wk, 42.50.Pq

## I. INTRODUCTION

Quantum mechanics dictates that no matter or field can stay absolutely at rest, even at the ground state, for which energy is at minimum. A starting point for deducing this inevitable fluctuation is to write down the Heisenberg uncertainty principle

$$[\hat{x}, \hat{p}] = i\hbar, \quad (1)$$

which leads to

$$\Delta x \Delta p \geq \hbar/2. \quad (2)$$

Here  $\hat{x}$  and  $\hat{p}$  are the position and momentum operators, while  $\Delta x$  and  $\Delta p$  are the standard deviations of position and momentum for an arbitrary quantum state. Equation (2) means that we cannot specify the position and momentum of a harmonic oscillator simultaneously as a point in classical phase space—the oscillator must at least occupy  $\hbar/2$  area in the phase space. If the oscillator has mass of  $m$  and eigenfrequency of  $\omega_m$ , then in the Heisenberg picture we can write

$$[\hat{x}_q(t), \hat{x}_q(t')] = \frac{i\hbar \sin \omega_m(t' - t)}{m\omega_m}, \quad (3)$$

which leads to

$$\Delta x_q(t) \Delta x_q(t') \geq \frac{\hbar |\sin \omega_m(t' - t)|}{2m\omega_m}, \quad (4)$$

with  $\hat{x}_q(t)$  being the Heisenberg operator of the oscillator position, quantum mechanically evolving under the free Hamiltonian. Here  $\Delta x_q(t)$  is the standard deviation of  $\hat{x}_q(t)$  for an arbitrary quantum state. Equation (4) means that the position of a freely evolving quantum harmonic oscillator cannot continuously assume precise values, but instead must fluctuate. This fluctuation carries the zero-point mechanical energy of  $\hbar\omega_m/2$ .

As a key feature of quantum mechanics, the zero-point fluctuation of displacement is an important effect to verify when we bring macroscopic mechanical degrees of freedom into their ground states [1–8]. Needless to say, a continuous observation of the zero-point fluctuation of a macroscopic mechanical oscillator requires superb displacement sensitivity.

However, what constitutes an “observation of the quantum zero-point fluctuation” is conceptually subtle. Equations (3) and (4), which argue for the inevitability of the zero-point fluctuation, also dictate that the “exact amount” of the zero-point fluctuation cannot be determined precisely. More specifically, if we use a linear measurement device to probe the zero-point fluctuation, which has an output field of  $\hat{y}(t)$ , then we must at least have

$$[\hat{y}(t), \hat{y}(t')] = 0 \quad (5)$$

at all times in order for  $\hat{y}(t)$  to be able to represent an experimental data string—with measurement noise simply due to the projection of the device’s quantum state into simultaneous eigenstates of all  $\{\hat{y}(t) : t \in \mathbb{R}\}$ . This means  $\hat{y}$  must be written as

$$\hat{y}(t) = \hat{\epsilon}(t) + \hat{x}_q(t), \quad (6)$$

with nonvanishing additional noise (error)  $\hat{\epsilon}(t)$ , which consists of degrees of freedom of the measurement device and compensates the nonvanishing commutator of  $\hat{x}_q$ .<sup>1</sup> In addition, during the measurement process, the actual evolution of the mechanical displacement  $\hat{x}$  must differ from its free evolution  $\hat{x}_q$ . This is because

$$\frac{[\hat{x}(t), \hat{x}(t')]}{i\hbar} \equiv \chi(t' - t) \quad (7)$$

is also the classical response function of  $x$  to an external force: any device that attempts to measure  $\hat{x}$  by coupling it with an external observable  $\hat{F}$ , which introduces a term proportional to  $\hat{x} \hat{F}$  into the Hamiltonian, will have to cause nonzero disturbance. For this reason, we can expand the measurement error  $\hat{\epsilon}$  into two parts, i.e.,  $\hat{z}$  is the sensing

<sup>1</sup>We note that Ozawa has developed a different formalism to quantify the issues that arise when attempts are made to measure noncommuting observables such as  $\hat{x}_q(t)$  [9,10]. However, we have chosen to adopt the Braginsky-Khalili approach [11] because it is immediately applicable when the noncommuting observable is acting as a probe for an external classical force.

noise that is independent from mechanical motion and  $\hat{x}_{\text{BA}}$  is additional disturbance to the mechanical motion from the measurement-induced back-action, and rewrite  $\hat{y}(t)$  as

$$\hat{y}(t) = \underbrace{\hat{z}(t) + \hat{x}_{\text{BA}}(t)}_{\hat{\epsilon}(t)} + \hat{x}_q(t) = \hat{z}(t) + \hat{x}(t). \quad (8)$$

The mechanical displacement under measurement is therefore a sum of the freely evolving operator  $\hat{x}_q$  plus the disturbance  $\hat{x}_{\text{BA}}$  due to back-action noise, namely,  $\hat{x}(t) = \hat{x}_q(t) + \hat{x}_{\text{BA}}(t)$ .

The above lines of reasoning lie very much at the heart of linear quantum measurement theory, pioneered by Braginsky in the late 1960s, aiming to describe resonant-bar gravitational-wave detectors [11,12] and later adapted to the analysis of laser interferometer gravitational-wave detectors by Caves [13]. A key concept in linear quantum measurement theory is the trade-off between sensing noise and back-action noise, which gives rise to the so-called standard quantum limit (SQL). For optomechanical devices, sensing noise takes the form of quantum shot noise due to the discreteness of photons, while the quantum back-action is enforced by quantum fluctuations in the radiation pressure acting on the mechanical oscillators [13], which is therefore also called quantum radiation-pressure noise. It has been shown that the SQL, although not a strict limit for sensitivity, can only be surpassed by carefully designed linear measurement devices, which take advantage of quantum correlations between the sensing noise and the back-action noise.

Observing signatures of quantum back-action, achieving and surpassing the associated SQL in mechanical systems are of great importance for the future of quantum-limited metrology, e.g., gravitational-wave detections [14–22]. At the moment, it is still experimentally challenging to directly observe quantum radiation-pressure noise in optomechanical devices due to high levels of environmental thermal fluctuations, and there are significant efforts being made toward this [4–8,23]. One approach proposed by Verlot *et al.* [4] is, instead, to probe the quantum correlation between the shot noise and the radiation-pressure noise, which, in principle, is totally immune to thermal fluctuations.

In this paper, we analyze a recent experiment performed by Safavi-Naeini *et al.* [24] in which a radiation-pressure-cooled nanomechanical oscillator—the movable mirror of a high-finesse cavity—is probed by a second beam of light, detuned from the cavity, for its zero-point mechanical oscillation. The output power spectrum of the second beam, near the mechanical resonant frequency, serves as an indicator of the oscillator’s zero-point motion. It was experimentally observed that when the second beam is detuned on opposite sides from the cavity resonance, the output power spectra turn out to be different. By using the theory of linear quantum measurements, we will show that this experiment not only probes the zero-point fluctuation of the mechanical oscillator at nearly ground state, but also illustrates vividly the nontrivial correlations between sensing noise and back-action noise—a much sought-after effect in the gravitational-wave-detection community. *Its contribution to the output spectrum is equal to the zero-point fluctuation for one detuning of the readout beam, and exactly opposite for the other detuning.*

The outline of this paper is as follows: In Sec. II, we will give a brief overview of the experiment by Safavi-Naeini *et al.* and present an analysis of this experiment using quantum measurement theory. In Sec. III, we will more broadly discuss the nature of the mechanical zero-point fluctuation, and show that in attempts to measure the zero-point fluctuation, the contributions from sensing–back-action noise correlations can generically be comparable to the zero-point fluctuation itself. In addition, we will discuss linear quantum measurement devices that use a near-ground-state mechanical oscillator as a probe for external classical forces near its resonant frequency, and show the limitation on the measurement sensitivity imposed by the zero-point fluctuation and the connection to the SQL. We will conclude in Sec. IV.

## II. A TWO-BEAM EXPERIMENT THAT MEASURES ZERO-POINT MECHANICAL OSCILLATION

We describe in Sec. II A the experiment performed by Safavi-Naeini *et al.*, put its results into the framework of linear quantum measurement theory in Sec. II B, and provide a detailed analysis in Sec. II C. In Sec. II D, we comment on the connection between the viewpoint from quantum measurement and the scattering picture presented in Ref. [24].

### A. Experimental setup and results

In the experiment, two spatial optical modes are coupled to a mechanical vibrational mode in a patterned silicon nanobeam. One spatial mode—the cooling mode—is pumped with a relatively high power at a “red” detuning (lower than resonance), and is used to cool the mechanical mode via radiation pressure damping [2]; the other cavity mode—the readout mode—has a much lower power and is used for probing the mechanical motion. The readout laser frequency  $\omega_{lr}$  is detuned from the resonant frequency  $\omega_r$  of the readout mode by either  $+\omega_m$  or  $-\omega_m$ . The observed spectra of the readout laser are asymmetric with respect to the detuning,  $\Delta \equiv \omega_r - \omega_{lr}$ . Specifically, in the positive-detuning case,  $\Delta = \omega_m$ , the spectrum has a smaller amplitude than that in the negative-detuning case. The area  $I_+$  enclosed by the spectrum in the positive-detuning case, *after subtracting out the noise floor away from the mechanical resonant frequency*, is proportional to the thermal occupation number  $\langle n \rangle$  of the mechanical oscillator, while in the negative-detuning case, the enclosed area is  $I_- \propto \langle n \rangle + 1$ . Such asymmetry is illustrated in Fig. 1. In Ref. [24], we introduced the following figure of

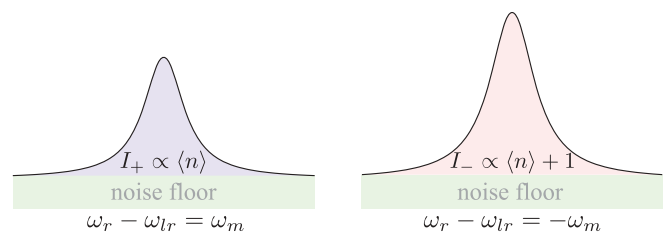


FIG. 1. (Color online) The observed spectra of the readout laser in the positive-detuning case (left) and the negative-detuning case (right).

merit to quantify the asymmetry:

$$\eta \equiv \frac{I_-}{I_+} - 1 = \frac{1}{\langle n \rangle}. \quad (9)$$

We interpreted this asymmetry as arising from the quantized motion of the mechanical oscillator. The asymmetry is thus assigned to the difference between the phonon absorption rate, proportional to  $\langle n \rangle$ , and the emission rate, proportional to  $\langle n \rangle + 1$ . This is completely analogous to that used for the calibration of the motional thermometry of ions (atoms) trapped in electrical (optical) traps [25–28]. Additionally, these scattering processes have an underlying physics similar to the bulk nonlinear Raman-scattering processes used in the spectroscopic analysis of crystals [29,30], where an ensemble of vibrational degrees of freedom internal to the molecular structure of the system interacts with incident light. Typically, in these nonlinear optics experiments, photon counters are used to keep track of the (anti-)Stokes photons. In contrast, in our experiment, a heterodyne measurement scheme was used to find the amplitude quadrature of the readout mode. Interestingly, by choosing the detuning  $\Delta = \pm\omega_m$ , and in the resolved-sideband regime, spectra of the amplitude quadrature are equal to the emission spectra of the (anti-)Stokes photons plus a constant noise floor due to vacuum fluctuation of the light—the shot noise. We will elaborate on this point in Sec. II D and show explicitly such a connection. Intuitively, one can view the cavity mode as an optical filter to selectively measure the emission spectra—for  $\Delta = \omega_m$ , the anti-Stokes process is significantly enhanced as the emitted photon is on resonance with respect to the cavity mode, and one therefore measures the spectrum for the anti-Stokes photons; while for  $\Delta = -\omega_m$ , the spectrum of the Stokes photon is measured.

### B. Interpretation in terms of quantum measurement

Here we provide an alternative viewpoint to Ref. [24], emphasizing the role of quantum back-action and its relation to quantization of the mechanical oscillator. First of all, we separate the experimental system into two parts. The first part includes the cooling mode, the mechanical oscillator, and the environmental thermal bath that the oscillator couples to (the left and middle boxes in Fig. 2), which can be viewed as providing an *effective mechanical oscillator* nearly at the ground state, but with a quality factor significantly lower than the intrinsic quality factor of the mechanical mode. It is the zero-point fluctuation of this effective oscillator that we shall be probing. The second part of the system consists of the readout mode (the box on the right of Fig. 2), which couples to the effective oscillator (the first part of the system) through displacement  $\hat{x}$  alone. The second part provides us with an output  $\hat{y}$ , which contains information about the zero-point fluctuation of the effective mechanical oscillator.



FIG. 2. (Color online) The relation among different parts of the optomechanical system in the experiment. The thermal heat bath and the cooling mode together create an effective quantum heat bath for the mechanical oscillator, which in turn couples to the readout mode.

### 1. The mechanical oscillator near ground state

Let us focus on the first part of the system (left two boxes of Fig. 2), namely, the effective mechanical oscillator (since this will be a stand-alone subject of study in later discussions, we shall often ignore the word “effective”). The environmental heat bath and the cooling mode together form a *quantum* heat bath with fluctuation close to the zero-point value. In the steady state, the “free” mechanical displacement is determined by its coupling to this bath (“free” means the absence of the readout mode):

$$\hat{x}_q(t) = \int_{-\infty}^t \chi(t-t') \hat{F}_q(t') dt'. \quad (10)$$

Here  $\chi$  is the response function of the mechanical oscillator, and for a high-quality-factor oscillator, we have

$$\chi(t-t') = -\frac{[\hat{x}(t), \hat{x}(t')]}{i\hbar} = e^{-\kappa_m |t-t'|/2} \frac{\sin \omega_m(t-t')}{m\omega_m}. \quad (11)$$

Note that we have an additional decay factor compared with Eq. (3), which describes an *idealized* free oscillator. The decay rate  $\kappa_m$  here is determined jointly by the intrinsic decay rate of the mechanical mode, and the optomechanical interaction between the mechanical mode and the cooling mode. The force  $\hat{F}_q$  lumps together the fluctuating force acting on the mechanical mode by the environmental heat bath and the cooling mode. If the oscillator approaches the ground state only after applying the cooling mode, then one can show that  $\hat{F}_q$  is dominated by fluctuation of the cooling mode.

The above two equations state that for a realistic mechanical oscillator with nonzero decay rate, its zero-point fluctuation in the steady state can be viewed as driven by the quantum heat bath surrounding it. We will return to this prominent feature of linear quantum systems later in Sec. III A.

### 2. The quantum measurement process

Let us now move on to the second part of the system (right box of Fig. 2), in which the readout mode serves as a linear position meter that measures the mechanical displacement. We can rewrite the disturbance  $\hat{x}_{BA}$  in Eq. (8) in terms of the back-action force  $\hat{F}_{BA}$  arising from the radiation-pressure fluctuation of the readout mode, namely,

$$\hat{x}_{BA}(t) = \int_{-\infty}^t \chi(t-t') \hat{F}_{BA}(t') dt'. \quad (12)$$

We have assumed that the readout mode does not modify the dynamics of the oscillator, which is a good approximation for the low pumping power used in the experiment. Written in the frequency domain, the readout mode output  $\hat{y}$  [cf. Eq. (8)] is

$$\hat{y}(\omega) = \hat{z}(\omega) + \chi(\omega) \hat{F}_{BA}(\omega) + \chi(\omega) \hat{F}_q(\omega), \quad (13)$$

where

$$\chi(\omega) = -\frac{1}{m(\omega^2 - \omega_m^2 + i\kappa_m\omega)} \quad (14)$$

is the Fourier transform of  $\Theta(t)\chi(t)$ , with  $\Theta$  the Heaviside function, i.e., the positive half of  $\chi(t)$  [even though  $\chi(t)$  exists for both  $t > 0$  and  $t < 0$ ]. The spectral density  $S_{yy}(\omega)$  of  $\hat{y}$  then reads

$$S_{yy} = S_{zz} + 2\text{Re}[\chi^* S_{zF}] + |\chi|^2 S_{FF}^{BA} + |\chi|^2 S_{FF}^q. \quad (15)$$

Here these single-sided spectral densities are defined in a symmetrized way (see Appendix A), which guarantees bilinearity for the cross spectrum and positivity for the self-spectrum.  $S_{zz}$  and  $S_{FF}^{\text{BA}}$  are the sensing-noise and back-action force noise spectra, respectively;  $S_{zF}$  is the cross correlation between  $\hat{z}$  and  $\hat{F}_{\text{BA}}$ ; and the force spectrum of the effective quantum heat bath made up by the environmental heat bath and the cooling mode is given by

$$S_{FF}^q = (4\langle n \rangle + 2)\hbar m \kappa_m \omega_m, \quad (16)$$

where  $\langle n \rangle$  is the thermal occupation number.

### 3. Asymmetry between spectra

Experimentally, it was observed that the output spectra  $S_{yy}$  for the two opposite detunings,  $\Delta = \pm\omega_m$ , are different—given the same thermal occupation number for the oscillator,

$$S_{yy}(\omega)|_{\Delta=-\omega_m} \neq S_{yy}(\omega)|_{\Delta=\omega_m}. \quad (17)$$

As we will show in Sec. II C, when we flip the sign of the detuning  $\Delta$  of the readout beam, the only term in  $S_{yy}$  that changes is  $S_{zF}$ , which is the correlation between the sensing noise and the back-action noise. According to Eq. (34), we have

$$S_{zF}(\omega) \approx -i\hbar \frac{\omega}{\Delta} \quad (18)$$

in the resolved-sideband regime with the cavity bandwidth  $\kappa_r \ll \omega_m$ , which is the case in the experiment. The asymmetry factor defined in Eq. (9) is given by

$$\eta = \frac{2 \int \text{Re}[\chi^*(S_{zF}^- - S_{zF}^+)]d\omega}{\int [|\chi|^2 S_{FF}^q + 2\text{Re}(\chi^* S_{zF}^+)]d\omega} = \frac{1}{\langle n \rangle}. \quad (19)$$

Here  $S_{zF}^\pm$  is defined by  $S_{zF}^\pm \equiv S_{zF}|_{\Delta=\pm\omega_m}$ , and in particular around the mechanical resonant frequency  $\omega_m$ , where  $S_{zF}^\pm$  contribute to the above integral,

$$S_{zF}^\pm \approx \mp i\hbar. \quad (20)$$

The asymmetry, or effect of quantum correlation  $S_{zF}$ , is most prominent when the thermal occupation number approaches zero. Indeed, if we focus on the quantum fluctuation by taking the limit of  $\langle n \rangle \rightarrow 0$ , then we obtain

$$\int 2\text{Re}(\chi^* S_{zF}^\pm)d\omega = \mp \int |\chi|^2 S_{FF}^q|_{\langle n \rangle=0}d\omega. \quad (21)$$

In other words, at the quantum ground state, the contribution of the quantum correlation  $S_{zF}$  to the readout spectrum  $S_{yy}$  has the same magnitude as that of the zero-point fluctuation, while the sign of the correlation term depends on the sign of the detuning of the readout beam. *This means that not only has the experiment probed the zero-point fluctuation of the mechanical oscillator, but it has also demonstrated nontrivial correlations between the sensing noise and back-action noise at the quantum level.*

### C. Detailed theoretical analysis

In this section, we supply a detailed calculation of the quantum dynamics and the output spectrum of the experiment. The dynamics for a typical linear optomechanical device has

been studied extensively in the literature [31–33]; however, the focus has been on the quantum state of the mechanical oscillator in ground-state cooling experiments, instead of treating the optomechanical device as a measurement device. Here we will follow Ref. [34] and derive the corresponding input-output relation—the analysis is the same as that of quantum noise in a detuned signal-recycling laser interferometer, which can be mapped into a detuned cavity [15,35,36]. We will focus only on the interaction between the readout cavity mode and the mechanical oscillator—the cooling mode and the thermal heat bath are taken into account by the effective dynamics of the oscillator, as mentioned earlier.

The Hamiltonian of our optomechanical system can be written as [31–33]

$$\hat{\mathcal{H}} = \hbar \omega_r \hat{a}^\dagger \hat{a} + \hat{\mathcal{H}}_{\kappa_r} + \hbar G_0 \hat{x} \hat{a}^\dagger \hat{a} + \frac{\hat{p}^2}{2m} + \frac{1}{2} m \omega_m^2 \hat{x}^2 + \hat{\mathcal{H}}_{\kappa_m}. \quad (22)$$

Here the first two terms describe the cavity mode including its coupling to the external continuum, the third term is the coupling between the cavity mode and the mechanical oscillator,  $G_0 = \omega_r/L_c$  is the coupling constant with  $L_c$  the cavity length, and the rest of the terms describe the dynamics of the effective oscillator (left and middle boxes in Fig. 2), with  $\hat{\mathcal{H}}_{\kappa_m}$  summarizing the dynamics of the cooling mode and the thermal heat bath, as well as their coupling with the original mechanical oscillator.

In the rotating frame at the laser frequency, the *linearized* equations of motion for the perturbed part—the variation around the steady-state amplitude—read

$$m(\ddot{\hat{x}} + \kappa_m \dot{\hat{x}} + \omega_m^2 \hat{x}) = \hat{F}_{\text{BA}} + \hat{F}_q, \quad (23)$$

$$\dot{\hat{a}} + (\kappa_r/2 + i\Delta)\hat{a} = -i\bar{G}_0 \hat{x} + \sqrt{\kappa_r} \hat{a}_{\text{in}}, \quad (24)$$

where the back-action force  $\hat{F}_{\text{BA}}$  is defined as

$$\hat{F}_{\text{BA}} \equiv -\hbar \bar{G}_0 (\hat{a} + \hat{a}^\dagger), \quad (25)$$

and we introduce  $\bar{G}_0 = \bar{a} G_0$ , where  $\bar{a}$  is the steady-state amplitude of the cavity mode and  $\hat{a}_{\text{in}}$  is the annihilation operator of the input vacuum field. The cavity output  $\hat{a}_{\text{out}}$  is related to the cavity mode by

$$\hat{a}_{\text{out}} = -\hat{a}_{\text{in}} + \sqrt{\kappa_r} \hat{a}, \quad (26)$$

with  $\kappa_r$  the decay rate (the bandwidth) of the readout mode.

In the steady state, these equations of motion can be solved more easily in the frequency domain. Starting from the mechanical displacement, we get

$$\hat{x}(\omega) = \chi(\omega) [\hat{F}_{\text{BA}}(\omega) + \hat{F}_q(\omega)]. \quad (27)$$

Here we have ignored the modification to the mechanical response function  $\chi$  due to the readout mode—a term proportional to  $\bar{G}_0^2$ , assuming that the pumping power is low. For the cavity mode, we invert Eq. (24) and obtain

$$\hat{a}(\omega) = \frac{\bar{G}_0 \hat{x}(\omega) + i\sqrt{\kappa_r} \hat{a}_{\text{in}}(\omega)}{\omega - \Delta + i\kappa_r/2}, \quad (28)$$

which leads to

$$\hat{F}_{\text{BA}}(\omega) = \frac{2\hbar \bar{G}_0 \sqrt{\kappa_r} / 2 [(\kappa_r/2 - i\omega)\hat{v}_1 + \Delta \hat{v}_2]}{(\omega - \Delta + i\kappa_r/2)(\omega + \Delta + i\kappa_r/2)}, \quad (29)$$

with  $\hat{v}_1 \equiv (\hat{a}_{\text{in}} + \hat{a}_{\text{in}}^\dagger)/\sqrt{2}$  and  $v_2 \equiv (\hat{a}_{\text{in}} - \hat{a}_{\text{in}}^\dagger)/(\sqrt{2}i)$  being the amplitude quadrature and the phase quadrature of the input field, which has fluctuations at the vacuum level. When combining with Eq. (26), we obtain the output amplitude quadrature

$$\begin{aligned} \hat{Y}_1(\omega) &= [\hat{a}_{\text{out}}(\omega) + \hat{a}_{\text{out}}^\dagger(-\omega)]/\sqrt{2} \\ &= \frac{(\Delta^2 - \kappa_r^2/4 - \omega^2)\hat{v}_1 - \kappa_r \Delta \hat{v}_2 + \sqrt{2\kappa_r} \bar{G}_0 \Delta \hat{x}}{(\omega - \Delta + i\kappa_r/2)(\omega + \Delta + i\kappa_r/2)}, \end{aligned} \quad (30)$$

whose spectrum is measured experimentally. We put the above formula into the same format as Eq. (13) by normalizing  $\hat{Y}_1$  with respect to the mechanical displacement  $\hat{x}$ , and introduce  $\hat{y}(\omega)$  and the corresponding sensing noise  $\hat{z}(\omega)$ :

$$\begin{aligned} \hat{y}(\omega) &= \frac{(\Delta^2 - \kappa_r^2/4 - \omega^2)\hat{v}_1 - \kappa_r \Delta \hat{v}_2}{\sqrt{2\kappa_r} \bar{G}_0 \Delta} + \hat{x}(\omega) \\ &\equiv \hat{z}(\omega) + \chi(\omega)[\hat{F}_{\text{BA}}(\omega) + \hat{F}_q(\omega)]. \end{aligned} \quad (31)$$

Taking the single-sided symmetrized spectral density of  $\hat{y}$  (see Appendix A), we obtain

$$S_{yy}(\omega) = S_{zz} + 2\text{Re}[\chi^* S_{zF}] + |\chi|^2 [S_{FF}^{\text{BA}} + S_{FF}^q], \quad (32)$$

where

$$S_{zz}(\omega) = \frac{(\Delta^2 - \kappa_r^2/4 - \omega^2)^2 + \kappa_r^2 \Delta^2}{2\kappa_r \bar{G}_0^2 \Delta^2}, \quad (33)$$

$$S_{zF}(\omega) = \frac{\hbar(\kappa_r/2 - i\omega)}{\Delta}, \quad (34)$$

$$S_{FF}^{\text{BA}}(\omega) = \frac{2\hbar^2 \bar{G}_0^2 \kappa_r (\kappa_r^2/4 + \omega^2 + \Delta^2)}{(\Delta^2 - \kappa_r^2/4 - \omega^2)^2 + \kappa_r^2 \Delta^2}. \quad (35)$$

Here we have used

$$\langle 0 | \hat{v}_j(\omega) \hat{v}_k^\dagger(\omega') | 0 \rangle_{\text{sym}} = \pi \delta_{jk} \delta(\omega - \omega') \quad (j, k = 1, 2). \quad (36)$$

Indeed, only  $S_{zF}$  depends on the sign of detuning and contributes to the asymmetry. In the resolved-sideband case  $\kappa_r \ll \omega_m$  and choosing detuning  $|\Delta| = \omega_m$ ,  $S_{zF}$  can be approximated as the one shown in Eq. (18). For a weak readout beam, we can ignore  $S_{FF}^{\text{BA}}$ , which is proportional to  $\bar{G}_0^2$ , and the output spectra around  $\omega_m$  for the positive- and negative-detuning cases can be approximated as

$$S_{yy}(\omega)|_{\Delta=\pm\omega_m} \approx \frac{\kappa_r}{2\bar{G}_0^2} + \frac{\hbar\kappa_m(2\langle n \rangle + 1 \mp 1)}{2m\omega_m[(\omega - \omega_m)^2 + (\kappa_m/2)^2]}. \quad (37)$$

As we can see, the contribution to output spectra from the quantum correlation has the same magnitude as the zero-point fluctuation of the mechanical oscillator, with a sign depending on the detuning. One can then obtain the dependence of the asymmetry factor  $\eta$  on  $\langle n \rangle$ , as shown in Eq. (9).

Interestingly, even if the quantum back-action term  $S_{FF}^{\text{BA}}$  is much smaller than  $S_{FF}^q$  and has been ignored, given the weak readout mode used in the experiment, the asymmetry induced by quantum correlation is always visible as long as  $\langle n \rangle$  is small. In addition, any optical loss in the readout mode only contributes a constant noise background—that is symmetric with respect to detuning—to the overall spectrum; therefore,

the asymmetry is very robust against optical loss, and it can be observed without a quantum-limited readout mode, which is the case in the experiment.

#### D. Connection with the scattering picture

In the above, we have been emphasizing the viewpoint of position measurement and interpreting the asymmetry as due to the quantum correlation between the sensing noise and the back-action noise. Here we would like to show the connection between this viewpoint and the scattering picture in Ref. [24] that focuses on the photon-phonon coupling, and, in addition, show how the spectra of the amplitude quadrature measured in the experiment are related to the emission spectra of the (anti-)Stokes photons that would be obtained if we instead take a photon-counting measurement.

To illustrate these, we introduce the annihilation operator  $\hat{b}$  for the phonon through the standard definition,

$$\hat{x} \equiv \sqrt{\hbar/(2m\omega_m)}(\hat{b} + \hat{b}^\dagger), \quad (38)$$

and it satisfies the commutator relation  $[\hat{b}, \hat{b}^\dagger] = 1$ . In the rotating frame at the laser frequency, the Hamiltonian in Eq. (22) after linearization is given by

$$\hat{\mathcal{H}} = \hbar\Delta\hat{a}^\dagger\hat{a} + \hat{\mathcal{H}}_{\kappa_r} + \hbar\bar{g}_0(\hat{a} + \hat{a}^\dagger)(\hat{b} + \hat{b}^\dagger) + \hbar\omega_m\hat{b}^\dagger\hat{b} + \hat{\mathcal{H}}_{\kappa_m}, \quad (39)$$

where  $\bar{g}_0 \equiv \bar{G}_0\sqrt{\hbar/(2m\omega_m)}$ . The third term is the photon-phonon coupling:  $\hat{a}^\dagger\hat{b}$  describes the anti-Stokes process where the absorption of a phonon is accompanied by the emission of a higher-frequency photon, and  $\hat{a}^\dagger\hat{b}^\dagger$  describes the Stokes process where the emission of a phonon is accompanied by the emission of a lower-frequency photon. The photon emission rate of these two processes can be estimated by using the *Fermi's golden rule*. Specifically, taking into account the finite bandwidth for the photon and phonon due to coupling to the continuum, the emission rate of the anti-Stokes photon at  $\omega_l + \omega$  reads

$$\begin{aligned} \Gamma_{AS}(\omega) &= \bar{g}_0^2 \int d\tau e^{i\omega\tau} \mathcal{D}(\omega) \langle \hat{b}^\dagger(\tau) \hat{b}(0) \rangle \\ &= \frac{\bar{g}_0^2 \kappa_m \langle n \rangle \mathcal{D}(\omega)}{(\omega - \omega_m)^2 + (\kappa_m/2)^2}, \end{aligned} \quad (40)$$

and the emission rate of the Stokes photon at  $\omega_l - \omega$  reads

$$\begin{aligned} \Gamma_S(\omega) &= \bar{g}_0^2 \int d\tau e^{-i\omega\tau} \mathcal{D}(-\omega) \langle \hat{b}(\tau) \hat{b}^\dagger(0) \rangle \\ &= \frac{\bar{g}_0^2 \kappa_m (\langle n \rangle + 1) \mathcal{D}(-\omega)}{(\omega - \omega_m)^2 + (\kappa_m/2)^2}. \end{aligned} \quad (41)$$

Here the density of state for the photons is determined by the cavity decay rate and detuning:

$$\mathcal{D}(\omega) \equiv \frac{\kappa_r/2}{(\omega - \Delta)^2 + (\kappa_r/2)^2}. \quad (42)$$

Were the cavity bandwidth much larger than the mechanical frequency  $\omega_m$ , the density of state  $\mathcal{D}(\omega)$  would become flat for frequencies around  $\pm\omega_m$ , and we would effectively have a scenario that is similar to the free-space Raman scattering as in those spectroscopic measurements of crystals [30]. By making a photon-counting-type measurement of the emitted

(anti-)Stokes photons, one could observe an asymmetric spectrum with two peaks (sidebands) around  $\omega_r \pm \omega_m$  of which the profiles are given by the above emission rates. This is also the case for those emission and absorption spectroscopic measurements in the ions and atoms trapping experiments [25–28].

The situation of our experiment is, however, different from the usual free-space Raman-scattering spectroscopic measurement by the following two aspects: (i) *We are operating in the resolved-sideband regime*, where the cavity bandwidth is much smaller than the mechanical frequency and the photon density of state is highly asymmetric for positive and negative sideband frequencies depending on the detuning. This basically dictates that we cannot measure two sidebands simultaneously, and we have to take two separate spectra by tuning the laser frequency. In the positive-detuning case  $\Delta = \omega_m$ , the anti-Stokes sideband is enhanced, while the Stokes sideband is highly suppressed, as the photon density of state is peak around  $\omega = \omega_m$ ; while in the negative-detuning case  $\Delta = -\omega_m$ , the situation for these two sidebands swaps. (ii) *We are using a heterodyne detection scheme instead of photon counting*, where the outgoing field is mixed with a large coherent optical field (reference light) before the photodetector, to measure the output amplitude quadrature, and the signal is linear proportional to the position of the oscillator, as we mentioned earlier. Interestingly, there is a direct connection between the spectra of amplitude quadrature measured in the experiment and the photon emission spectra that are obtained if making photon-counting measurements. To show this connection, we use the fact that

$$[\hat{Y}_1(\omega), \hat{Y}_1^\dagger(\omega')] = 0, \quad (43)$$

which is a direct consequence of  $[\hat{y}(t), \hat{y}(t')] = 0$  ( $\hat{y}$  is equal to  $\hat{Y}_1$  normalized with respect to the mechanical displacement [cf. Eq. (31)]), and we have

$$\begin{aligned} \langle \hat{Y}_1(\omega) \hat{Y}_1^\dagger(\omega') \rangle_{\text{sym}} &= \langle \hat{Y}_1^\dagger(\omega') \hat{Y}_1(\omega) \rangle \\ &= \frac{1}{2} [\langle \hat{a}_{\text{out}}(-\omega') \hat{a}_{\text{out}}^\dagger(-\omega) \rangle \\ &\quad + \langle \hat{a}_{\text{out}}^\dagger(\omega') \hat{a}_{\text{out}}(\omega) \rangle]. \end{aligned} \quad (44)$$

Take the positive-detuning case  $\Delta = \omega_m$ , for instance,  $\hat{a}_{\text{out}}(-\omega)$  contains mostly vacuum and negligible sideband signals due to suppression of the Stokes sideband around  $\omega_r - \omega_m$  by the cavity, namely,  $\langle \hat{a}_{\text{out}}(-\omega') \hat{a}_{\text{out}}^\dagger(-\omega) \rangle \approx 2\pi \delta(\omega - \omega')$ . The second term gives the emission spectrum for the output photons shown in Eq. (40); therefore, the single-sided spectral density of the output amplitude quadrature reads

$$S_{Y_1 Y_1}(\omega) = 1 + 2\Gamma_{\text{AS}}(\omega). \quad (45)$$

By normalizing the spectrum with respect to the mechanical displacement, we have

$$S_{yy}(\omega)|_{\Delta=\omega_m} = \frac{\kappa_r}{2\bar{G}_0^2} [1 + 2\Gamma_{\text{AS}}(\omega)]. \quad (46)$$

Similarly, by following the same line of thought, we get

$$S_{yy}(\omega)|_{\Delta=-\omega_m} = \frac{\kappa_r}{2\bar{G}_0^2} [1 + 2\Gamma_{\text{S}}(\omega)]. \quad (47)$$

The above two equations give identical results to Eq. (37). Therefore, the output spectra obtained in our heterodyne detection differ from those in the photon-counting measurement only by a constant noise floor, which originates from vacuum fluctuation of the amplitude quadrature. After subtracting this noise floor, we simply recover the emission spectra obtained from taking the photon-counting measurement.

### III. GENERAL LINEAR MEASUREMENTS OF THE ZERO-POINT FLUCTUATION

Based on the analysis of the specific experiment of Ref. [24] in the previous section, here we comment on the general features of linear quantum measurements involving reading out zero-point fluctuation of a mechanical oscillator. We start by discussing the nature of the zero-point mechanical fluctuation in Sec. III A, proceed to a discussion of the measurements of it in Sec. III B, and finally end in Sec. III C, which discusses its effect on sensitivity for measuring external forces and the connection to the SQL.

#### A. The nature of zero-point mechanical fluctuation

First of all, let us take a closer look at the nature of the zero-point fluctuation of a realistic harmonic oscillator, which consists of a mechanical mode with eigenfrequency  $\omega_m$  and finite decay rate  $\kappa_m$ . Suppose we initially decouple the oscillator from its environmental heat bath and turn on the coupling at  $t = 0$ . In the Heisenberg picture, the position and momentum of the oscillator at  $t > 0$  will be

$$\hat{x}_q(t) = \hat{x}_{\text{free}}(t) + \int_0^t \chi(t-t') \hat{F}_q(t') dt', \quad (48a)$$

$$\hat{p}_q(t) = \hat{p}_{\text{free}}(t) + m \int_0^t \dot{\chi}(t-t') \hat{F}_q(t') dt', \quad (48b)$$

where

$$\hat{x}_{\text{free}}(t) = e^{-\kappa_m t/2} \left[ \hat{x}(0) \cos \omega_m t + \frac{\hat{p}(0)}{m\omega_m} \sin \omega_m t \right], \quad (49a)$$

$$\begin{aligned} \frac{\hat{p}_{\text{free}}(t)}{m\omega_m} &= e^{-\kappa_m t/2} \left[ -\hat{x}(0) \sin \omega_m t + \frac{\hat{p}(0)}{m\omega_m} \cos \omega_m t \right] \\ &\quad - \frac{m\kappa_m}{2} \hat{x}_{\text{free}}(t), \end{aligned} \quad (49b)$$

are contributions from the free evolution of the initial Schrödinger operators (i.e., undisturbed by the environment), which decay over time and get replaced by contributions from the environmental heat bath [integrals on the right-hand side of Eqs. (48a) and (48b)]. Note that for any oscillator with nonzero decay rate, it is essential to have bath operators entering over time, otherwise the commutation relation between position and momentum,

$$[\hat{x}_q(t), \hat{p}_q(t)] = i\hbar, \quad (50)$$

will not hold at  $t > 0$  because of

$$[\hat{x}_{\text{free}}(t), \hat{p}_{\text{free}}(t)] = i\hbar e^{-\kappa_m t}. \quad (51)$$

This dictates that the heat bath must be such that the additional commutator from terms containing  $\hat{F}_q$  exactly compensates for the decay in Eq. (51), which leads to the quantum fluctuation-dissipation theorem (see, e.g., Ref. [37]).

It is interesting to note that this “replenishing” of commutators has a classical counterpart, since commutators are, after all, proportional to the classical Poisson bracket. More specifically, for a classical oscillator with decay, we can write a similar relation for Poisson brackets among the position and momentum of the oscillator, plus environmental degrees of freedom. The replenishing of the position-momentum Poisson bracket by environmental ones, in classical mechanics, can also be viewed as a consequence of the conservation of phase-space volume, following the Liouville theorem. A decaying oscillator’s phase-space volume will shrink and violate the Liouville theorem—unless additional phase-space volume from the environmental degrees of freedom is introduced.

Nevertheless, the definitive quantum feature in our situation is a fundamental scale in the volume of phase space, which is equal to  $\hbar$ . Here we note that if  $\kappa_m \ll \omega_m$ , when reaching the steady state with  $\hat{x}_{\text{free}}$  and  $\hat{q}_{\text{free}}$  decayed away, then we have

$$\Delta x_q \Delta p_q \approx m \omega_m \int \frac{d\omega}{2\pi} S_{xx}^q(\omega), \quad (52)$$

where  $S_{xx}^q \equiv |\chi|^2 S_{FF}^q$ . Although  $S_{xx}^q$  depends on the specific scenario, they are all constrained by a Heisenberg-like relation of

$$S_{xx}^q(\omega) \geq 2\hbar \text{Im}\chi(\omega), \quad (53)$$

which is a straightforward consequence of the commutation relation in Eq. (11). The equality is achieved at the ground state.<sup>2</sup> This enforces the same Heisenberg uncertainty relation,

$$\Delta x_q \Delta p_q \geq \hbar/2, \quad (54)$$

as an ideal harmonic oscillator whose quantum fluctuations arise “on their own,” instead of having to be driven by the surrounding environment. Therefore, in the steady state, the zero-point fluctuation of the mechanical oscillator can be viewed as being imposed by the environment due to the linearity of the dynamics.

### B. Measuring the zero-point fluctuation

Having clarified the nature of quantum zero-point fluctuations of a mechanical oscillator in the steady state, let us argue that the effects seen in Ref. [24] are actually generic when one tries to probe such fluctuations, namely: the correlation between sensing and back-action noise can be at the level of the zero-point fluctuation itself.

Let us start our discussion here from Eq. (5), namely,

$$[\hat{y}(t), \hat{y}(t')] = 0, \quad (55)$$

and the fact that  $\hat{y}$  consists of sensing noise, back-action noise, and finally the zero-point fluctuation of the mechanical oscillator [cf. Eq. (8)]:

$$\hat{y}(t) = \frac{\hat{z}(t)}{\alpha} + \alpha \int_{-\infty}^t \chi(t-\tau) \hat{F}_{\text{BA}}(\tau) d\tau + \hat{x}_q(t). \quad (56)$$

Here we have added a factor  $\alpha$ , which labels the scaling of each term as the measurement strength which is proportional to the

square root of the readout beam power. Let us assume that the dynamical response  $\chi$  of the oscillator is not modified due to couplings to the measurement field, and Eq. (55) continues to hold for the same set of  $\hat{z}$  and  $\hat{F}_{\text{BA}}$ , for a large set of  $\alpha$  and  $\chi$ : basically, the measuring device works for different mechanical oscillators with different measuring strength.

Since Eq. (55) remains valid for all values of  $\alpha$ , we extract terms with different powers of scaling, and obtain

$$[\hat{z}(t), \hat{z}(t')] = [\hat{F}_{\text{BA}}(t), \hat{F}_{\text{BA}}(t')] = 0, \quad (57)$$

and

$$\begin{aligned} & \int_{-\infty}^{t'} \chi(t'-\tau) [\hat{z}(t), \hat{F}_{\text{BA}}(\tau)] d\tau \\ & - \int_{-\infty}^t \chi(t-\tau) [\hat{z}(t'), \hat{F}_{\text{BA}}(\tau)] d\tau \\ & + [\hat{x}_q(t), \hat{x}_q(t')] = 0 \quad \forall t, t'. \end{aligned} \quad (58)$$

This becomes

$$\int_0^{+\infty} \chi(\tau) [C_{zF}(t-\tau) - C_{zF}(-t-\tau)] d\tau = -i\hbar\chi(t) \quad (59)$$

for all values of  $t$ , where we have defined

$$C_{zF}(t'-t) \equiv [\hat{z}(t), \hat{F}_{\text{BA}}(t')]. \quad (60)$$

Here the dependence is only through  $t' - t$  because the system is assumed to be time invariant. We also note that since  $\hat{z}$  is an outgoing field,  $C_{zF}(t' - t)$  must vanish when  $t' - t > 0$ , otherwise any generalized force applied on the outgoing field  $\hat{z}(t)$ , detached from the mechanical oscillator, can still dynamically influence the mechanical motion at later times (future) through  $\hat{F}_{\text{BA}}(t')$ , which violates the causality [11,35]. As proven in Appendix B, in order for Eq. (59) to be satisfied for all possible response functions of the oscillator, we must have

$$C_{zF}(t) = -i\hbar\delta_-(t), \quad (61)$$

where  $\delta_-(t)$  is the Dirac  $\delta$  function with support only for  $t < 0$ . In other words,

$$[\hat{z}(t), \hat{F}_{\text{BA}}(t')] = -i\hbar\delta_-(t' - t). \quad (62)$$

Equation (56), plus the commutation relations in Eqs. (57) and (62), then provide a general description of linear measuring devices, which do not modify the dynamics of the mechanical oscillator—simply from the requirement that the outgoing field operators at different times must commute [cf. Eq. (55)]. In particular, the nonvanishing commutator  $[\hat{x}_q(t), \hat{x}_q(t')]$ , which underlies the existence of the zero-point fluctuation, is canceled in a simple way by the nonvanishing commutator between the sensing noise and the back-action noise [cf. Eq. (62)].

Now turn to the noise content of the output  $\hat{y}(t)$ , i.e., the spectrum

$$S_{yy} = \frac{S_{zz}}{\alpha^2} + 2\text{Re}[\chi^* S_{zF}] + \alpha^2 S_{FF}^{\text{BA}} + S_{xx}^q. \quad (63)$$

Let us consider experiments with relatively low measurement strength, so that the first term  $S_{zz}/\alpha^2$  from the sensing noise dominates the output noise. The next-order terms contain (i) correlation between the sensing noise and the back-action

<sup>2</sup>A generalization of this to thermal states will be the fluctuation-dissipation theorem [37].

noise,  $S_{zF}$ ; and (ii) the mechanical fluctuation,  $S_{xx}^q$ . If we assume nearly ground state for the mechanical oscillator, then

$$S_{xx}^q(\omega) \approx 2\hbar \text{Im}\chi(\omega), \quad (64)$$

which, for  $\kappa_m \ll \omega_m$ , gives

$$\int \frac{d\omega}{2\pi} S_{xx}^q(\omega) \approx \frac{\hbar}{2m\omega_m}. \quad (65)$$

If  $S_{zF}(\omega)$  does not change noticeably within the mechanical bandwidth, then

$$\int \frac{d\omega}{2\pi} 2\text{Re}[\chi^*(\omega)S_{zF}(\omega)] \approx -\frac{1}{2m\omega_m} \text{Im}S_{zF}(\omega_m). \quad (66)$$

Because of Eq. (62), the typical magnitude for  $S_{zF}$  is naturally<sup>3</sup>

$$|S_{zF}| \sim \hbar. \quad (67)$$

Therefore, contributions to the output noise from quantum correlation  $S_{zF}$  and mechanical fluctuation  $S_{xx}^q$  can generically become comparable to each other when the mechanical oscillator is approaching the quantum ground state. The result presented in Ref. [24] therefore illustrates two typical cases of this generic behavior [cf. Eq. (20)].

### C. Measuring external classical forces in the presence of zero-point fluctuation

Finally, let us discuss the role of zero-point fluctuation in force measurement, when the mechanical oscillator is used as a probe of external classical forces not far away from the mechanical resonant frequency. The force sensitivity of such a linear measurement device, in terms of spectral density  $S_F$ , is obtained by normalizing the displacement sensitivity  $S_{yy}$  with respect to the mechanical response function  $\chi$ :  $S_F \equiv S_{yy}/|\chi|^2$ . Specifically, from Eq. (15), we have

$$S_F(\omega) = \frac{S_{zz}(\omega)}{|\chi(\omega)|^2} + 2\text{Re} \left[ \frac{S_{zF}(\omega)}{\chi(\omega)} \right] + S_{FF}^{\text{BA}}(\omega) + S_{FF}^q(\omega). \quad (68)$$

Because of the commutation relations in Eqs. (57) and (62), a Heisenberg uncertainty relation exists among the spectral densities of  $\hat{z}$  and  $\hat{F}_{\text{BA}}$ , which is

$$S_{zz}(\omega)S_{FF}^{\text{BA}}(\omega) - S_{zF}(\omega)S_{Fz}(\omega) \geq \hbar^2. \quad (69)$$

When the sensing noise  $\hat{z}$  and the back-action noise  $\hat{F}_{\text{BA}}$  are not correlated, i.e.,  $S_{zF} = S_{Fz} = 0$ , we have

$$S_{zz}(\omega)S_{FF}^{\text{BA}}(\omega) \geq \hbar^2. \quad (70)$$

The above inequality represents a trade-off between sensing noise  $\hat{z}$  and back-action noise  $\hat{F}_{\text{BA}}$ . Correspondingly, the force sensitivity will have a lower bound,

$$\begin{aligned} S_F(\omega)|_{S_{zF}=0} &= \frac{S_{zz}(\omega)}{|\chi(\omega)|^2} + S_{FF}^{\text{BA}}(\omega) + S_{FF}^q(\omega) \\ &\geq \frac{2\hbar}{|\chi(\omega)|} + (4\langle n \rangle + 2)\hbar m\kappa_m\omega_m. \end{aligned} \quad (71)$$

If the mechanical oscillator is in its quantum ground state, namely,  $\langle n \rangle = 0$ , then we obtain

$$S_F(\omega) \geq \frac{2\hbar}{|\chi(\omega)|} + 2\hbar m\kappa_m\omega_m \equiv S_F^{\text{Qtot}}. \quad (72)$$

The first term is the usual standard quantum limit (SQL) for force sensitivity with mechanical probes [11,12]:

$$S_F^{\text{SQL}} \equiv \frac{2\hbar}{|\chi(\omega)|} = 2\hbar m\sqrt{(\omega^2 - \omega_m^2)^2 + \kappa_m^2\omega^2}. \quad (73)$$

The second term,

$$S_F^{\text{zp}} \equiv 2\hbar m\kappa_m\omega_m, \quad (74)$$

arising from the zero-point fluctuation due to mechanical quantization, also limits the sensitivity. As we can learn from Eqs. (68), (69), and (72), the quantum limit can be surpassed, in principle, indefinitely by building up quantum correlations between the sensing noise  $\hat{z}$  and the back-action noise  $\hat{F}_{\text{BA}}$ ; in practice, the beating factor will be limited by the available optical power and the level of optical losses. However, the limit imposed by zero-point fluctuation cannot be surpassed and can only be mitigated by lowering  $\kappa_m$ , i.e., increasing the mechanical quality factor.

Braginsky *et al.* [38] argued that mechanical quantization does not influence the force sensitivity when measuring classical forces with mechanical probes—one only needs to evaluate the quantum noise due to the readout field. But these authors had specifically pointed out that they were focusing on ideal mechanical probes with infinitely narrow bandwidth ( $\kappa_m \rightarrow 0$ ) and observations outside of that frequency band. This is close to the actual situation of free-mass gravitational-wave detectors, in which the mechanical oscillator is the differential mode of four mirror-endowed test masses hung as pendulum with eigenfrequencies around 1 Hz and very high quality factor, while the detection band is above 10 Hz, which is well outside the mechanical resonance. Indeed, from Eqs. (73) and (74), we see that the effect of zero-point fluctuation is only significant not far away from resonance, which confirms Braginsky *et al.*'s result. More specifically, if  $\kappa_m \ll \omega_m$ , then we can write, for  $|\omega - \omega_m| \ll \omega_m$ ,

$$S_F^{\text{SQL}} \approx S_F^{\text{zp}} \sqrt{1 + \left( \frac{\omega - \omega_m}{\kappa_m/2} \right)^2}. \quad (75)$$

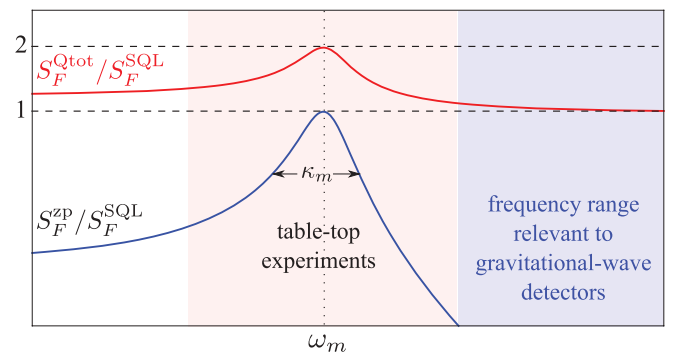


FIG. 3. (Color online) Total quantum limitation  $S_F^{\text{Qtot}}$  (upper red line) for force sensitivity and contribution from zero-point fluctuation  $S_F^{\text{zp}}$  (lower blue line). For clarity, we divide both by the SQL and use a log-log scale.

<sup>3</sup>In general, the commutator does not impose any bound on the cross correlation. Here, in a strict sense, is an order-of-magnitude estimate.



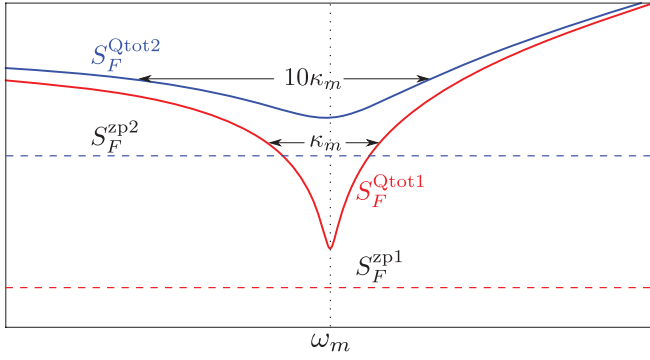


FIG. 4. (Color online) Effect of the mechanical decay rate (bandwidth)  $\kappa_m$  on  $S_F^{\text{Qtot}}$  (solid lines) and  $S_F^{\text{zp}}$  (dashed lines)—the larger the mechanical bandwidth, the lower the force sensitivity (this plot is also in the log-log scale).

In particular, the limit imposed by zero-point fluctuation is equal to SQL on resonance, and becomes less important as  $|\omega - \omega_m|$  becomes comparable to or larger than the half bandwidth  $\kappa_m/2$ , as illustrated in Fig. 3. Note that on an absolute scale,  $S_F^{\text{SQL}}(\omega)$  is lower near the mechanical resonance, while  $S_F^{\text{zp}}(\omega)$  is independent from frequency; at any frequency, lowering  $\kappa_m$ , while fixing  $\omega_m$  and keeping the oscillator at ground state, always results in lower noise, as illustrated in Fig. 4. Suppose we are free to choose from ground-state mechanical oscillators with different  $\omega_m$  and  $\kappa_m$  as our probe, and that we are always able to reach the SQL at all frequencies, then: (i) if we know the frequency content of the target signals, we can choose probes that are closely resonant with the target, and (ii) regardless of signal frequency, probes with lower  $\kappa_m$ , or equivalently, higher mechanical quality factor, always provide better force sensitivity.

#### IV. CONCLUSION

We have shown, within the framework of quantum measurement theory, that the asymmetry in the output spectra observed by Safavi-Naeini *et al.* can be explained as due to the quantum correlation between the sensing noise and the quantum back-action noise; this experiment therefore provides a clear signature of quantum back-action onto mechanical systems. More broadly, we have shown that having quantum-noise correlations showing up at the same level as the zero-point fluctuations is a generic feature of measurements that attempt to measure the zero-point fluctuation. We have further shown that when an experimentally prepared ground-state mechanical oscillator is used as a probe for classical forces near its resonant frequency, its mechanical quantization—through zero-point displacement fluctuation—does impose an addition noise background. This additional noise vanishes only if the oscillator's bandwidth approaches zero, i.e., when the oscillator becomes ideal.

#### ACKNOWLEDGMENTS

We thank A. Schliesser, M. Gorodetsky, and T. Kippenberg for fruitful discussions. F.Ya.K. is supported by the Russian

Foundation for Basic Research Grant No. 08-02-00580-a and NSF Grant No. PHY-0967049. H.M., H.Y., and Y.C. are supported by NSF Grants No. PHY-0555406, No. PHY-0956189, and No. PHY-1068881, as well as the David and Barbara Groce Startup Fund at Caltech. The research of A.S.-N. and O.P. has been supported by the DARPA/MTO ORCHID program through a grant from AFOSR, and the Kavli Nanoscience Institute at Caltech. A.S.-N. also gratefully acknowledges support from NSERC. We acknowledge funding provided by the Institute for Quantum Information and Matter, an NSF Physics Frontiers Center with support of the Gordon and Betty Moore Foundation.

#### APPENDIX A: SYMMETRIZED CROSS SPECTRAL DENSITY

In this paper, as in Ref. [14], we use the *single-sided* symmetrized cross spectral density, which, given a quantum state  $|\psi\rangle$ , is defined between a pair of operators  $\hat{A}$  and  $\hat{B}$  as

$$\begin{aligned} S_{AB}(\omega)\delta(\omega - \omega') &\equiv \frac{1}{\pi} \langle \psi | \hat{A}(\omega) \hat{B}^\dagger(\omega') | \psi \rangle_{\text{sym}} \\ &= \frac{1}{2\pi} \langle \psi | \hat{A}(\omega) \hat{B}^\dagger(\omega') + \hat{B}^\dagger(\omega') \hat{A}(\omega) | \psi \rangle. \end{aligned} \quad (\text{A1})$$

The symmetrization process here allows us to preserve the bilinearity of  $\hat{S}$  on its entries, i.e.,

$$S_{A, c_1 B + c_2 C} = c_1^* S_{AB} + c_2^* S_{AC}, \quad (\text{A2a})$$

$$S_{c_1 A + c_2 B, C} = c_1 S_{AC} + c_2 S_{BC}. \quad (\text{A2b})$$

More importantly, we can show that

$$S_{AA} > 0 \quad (\text{A3})$$

for any field  $\hat{A}$ , even if  $[\hat{A}(\omega), \hat{A}^\dagger(\omega')] \neq 0$ . The positivity (A3) allows us to interpret  $S_{AA}$  as the fluctuation variance per unit frequency band—as in the classical case.

#### APPENDIX B: COMMUTATION RELATION BETWEEN $\hat{z}$ AND $\hat{F}$

Defining

$$f(t) \equiv C_{zF}(t) + i\hbar\delta_-(t), \quad (\text{B1})$$

we convert Eq. (59) into

$$\int_0^{+\infty} \chi(\tau) [f(t - \tau) - f(-t - \tau)] d\tau = 0. \quad (\text{B2})$$

Assuming analyticity of the Fourier transform of  $f(t)$ , it must be written as

$$\tilde{f}(\omega) = \sum_k \frac{f_k}{\omega - \omega_k}, \quad (\text{B3})$$

with  $\omega_k$  all located on the upper half of the complex plane (not including the real axis). Fourier transforming Eq. (B2)

gives us

$$\tilde{\chi}_+(\omega) \sum_k \left[ \frac{f_k}{\omega - \omega_k} - \frac{f_k^*}{\omega - \omega_k^*} \right] = 0, \quad \omega \in \mathbb{R}. \quad (\text{B4})$$

Because the set  $\{\omega_k\}$  is within the upper-half complex plane (excluding the real axis), the set  $\{\omega_k^*\}$  must be within the lower-

half complex plane (excluding the real axis)—and the two sets do not intersect. For this reason, Eq. (B4) requires  $f_k$  to all vanish, and hence

$$C_{zF}(t) = -i\hbar \delta_-(t). \quad (\text{B5})$$

- 
- [1] T. J. Kippenberg and K. J. Vahala, *Science* **321**, 1172 (2008).
- [2] F. Marquardt and S. M. Girvin, *Physics* **2**, 40 (2009).
- [3] A. D. O’Connell, M. Hofheinz, M. Ansmann, R. C. Bialczak, M. Lenander, E. Lucero, M. Neeley, D. Sank, H. Wang, M. Weides *et al.*, *Nature (London)* **464**, 697 (2010).
- [4] P. Verlot, A. Tavernarakis, T. Briant, P.-F. Cohadon, and A. Heidmann, *Phys. Rev. Lett.* **102**, 103601 (2009).
- [5] J. D. Teufel, T. Donner, M. A. Castellanos-Beltran, J. W. Harlow, and K. W. Lehnert, *Nature Nanotechnol.* **4**, 820 (2009).
- [6] G. Anetsberger, O. Arcizet, Q. P. Unterreithmeier, R. Riviere, A. Schliesser, E. M. Weig, J. P. Kotthaus, and T. J. Kippenberg, *Nature Phys.* **5**, 909 (2009).
- [7] K. Børkje, A. Nunnenkamp, B. M. Zwickl, C. Yang, J. G. E. Harris, and S. M. Girvin, *Phys. Rev. A* **82**, 013818 (2010).
- [8] T. Westphal, D. Friedrich, H. Kaufer, K. Yamamoto, S. Göbner, H. Müller-Ebhardt, S. L. Danilishin, F. Y. Khalili, K. Danzmann, and R. Schnabel, *Phys. Rev. A* **85**, 063806 (2012).
- [9] M. Ozawa, *Phys. Rev. A* **67**, 042105 (2003).
- [10] J. Erhart, S. Sponar, G. Sulyok, G. Badurek, M. Ozawa, and Y. Hasegawa, *Nature Phys.* **8**, 185 (2012).
- [11] V. B. Braginsky and F. Y. Khalili, *Quantum Measurement* (Cambridge University Press, Cambridge, 1992).
- [12] V. B. Braginsky, *JETP* **26**, 831 (1968).
- [13] C. M. Caves, *Phys. Rev. Lett.* **45**, 75 (1980).
- [14] H. J. Kimble, Y. Levin, A. B. Matsko, K. S. Thorne, and S. P. Vyatchanin, *Phys. Rev. D* **65**, 022002 (2001).
- [15] A. Buonanno and Y. Chen, *Phys. Rev. D* **64**, 042006 (2001).
- [16] P. Purdue and Y. Chen, *Phys. Rev. D* **66**, 122004 (2002).
- [17] T. Corbitt, Y. Chen, F. Khalili, D. Ottaway, S. Vyatchanin, S. Whitcomb, and N. Mavalvala, *Phys. Rev. A* **73**, 023801 (2006).
- [18] T. Corbitt, Y. Chen, E. Innerhofer, H. Müller-Ebhardt, D. Ottaway, H. Rehbein, D. Sigg, S. Whitcomb, C. Wipf, and N. Mavalvala, *Phys. Rev. Lett.* **98**, 150802 (2007).
- [19] T. Corbitt, C. Wipf, T. Bodiya, D. Ottaway, D. Sigg, N. Smith, S. Whitcomb, and N. Mavalvala, *Phys. Rev. Lett.* **99**, 160801 (2007).
- [20] F. Marino, F. S. Cataliotti, A. Farsi, M. S. de Cumis, and F. Marin, *Phys. Rev. Lett.* **104**, 073601 (2010).
- [21] Y. Chen, S. L. Danilishin, F. Y. Khalili, and H. Müller-Ebhardt, *Gen. Rel. Grav.* **43**, 671 (2011).
- [22] S. L. Danilishin and F. Y. Khalili, *Living Rev. Relativity* **15**, 60 (2012).
- [23] K. Yamamoto, D. Friedrich, T. Westphal, S. Göbner, K. Danzmann, K. Somiya, S. L. Danilishin, and R. Schnabel, *Phys. Rev. A* **81**, 033849 (2010).
- [24] A. H. Safavi-Naeini, J. Chan, J. T. Hill, Thiago P. Mayer Alegre, A. Krause, and O. Painter, *Phys. Rev. Lett.* **108**, 033602 (2012).
- [25] F. Diedrich, J. C. Bergquist, W. M. Itano, and D. J. Wineland, *Phys. Rev. Lett.* **62**, 403 (1989).
- [26] P. S. Jessen, C. Gerz, P. D. Lett, W. D. Phillips, S. L. Rolston, R. J. C. Spreeuw, and C. I. Westbrook, *Phys. Rev. Lett.* **69**, 49 (1992).
- [27] C. Monroe, D. M. Meekhof, B. E. King, S. R. Jefferts, W. M. Itano, D. J. Wineland, and P. Gould, *Phys. Rev. Lett.* **75**, 4011 (1995).
- [28] N. Brahms, T. Botter, S. Schreppler, D. W. C. Brooks, and D. M. Stamper-Kurn, *Phys. Rev. Lett.* **108**, 133601 (2012).
- [29] T. R. Hart, R. L. Aggarwal, and B. Lax, *Phys. Rev. B* **1**, 638 (1970).
- [30] W. Hayes and R. Loudon, *Scattering of Light by Crystals* (Dover, New York, 2004).
- [31] F. Marquardt, J. P. Chen, A. A. Clerk, and S. M. Girvin, *Phys. Rev. Lett.* **99**, 093902 (2007).
- [32] I. Wilson-Rae, N. Nooshi, W. Zwerger, and T. J. Kippenberg, *Phys. Rev. Lett.* **99**, 093901 (2007).
- [33] C. Genes, D. Vitali, P. Tombesi, S. Gigan, and M. Aspelmeyer, *Phys. Rev. A* **77**, 033804 (2008).
- [34] H. Miao, S. Danilishin, H. Müller-Ebhardt, and Y. Chen, *New J. Phys.* **12**, 083032 (2010).
- [35] A. Buonanno and Y. Chen, *Phys. Rev. D* **65**, 042001 (2002).
- [36] A. Buonanno and Y. Chen, *Phys. Rev. D* **67**, 062002 (2003).
- [37] C. Gardiner and P. Zoller, *Quantum Noise* (Springer-Verlag Berlin, 2004).
- [38] V. B. Braginsky, M. L. Gorodetsky, F. Y. Khalili, A. B. Matsko, K. S. Thorne, and S. P. Vyatchanin, *Phys. Rev. D* **67**, 082001 (2003).